Journal of Applied Research and Technology

www.jart.icat.unam.mx

ICAT Instituto de Ciencias Aplicadas y Tecnología

Journal of Applied Research and Technology 24 (2026) 53-65

Original

Brushless D.C. motor drive control by using hybrid commutation

Sadhak Juli Singh[1*] • Bhusnur Surekha[2] • Dubey S.P[3]

[1]Research Scholar, Electrical Engineering Department, BIT Durg, Chhattisgarh, India
[2]Professor, EEE Department, BIT Durg, Chhattisgarh, India,
[3]Vice-Chancellor, ICFAI University Raipur, Chhattisgarh, India,

Received: 10 21 2024; Accepted: 03 06 2025
Available: 02 28 2026

Abstract: The permanent magnet brushless dc (BLDC) motor turned on and off by adjusting the magnetic fields created by the adjacent stationary coils in the appropriate direction. A BLDC motor's six terminals—two per coil—extend from the stator and can be used to regulate the motor's rotation. Feedback systems can be used to precisely control the torque and rotation speed of BLDC motors. There are two main types of three-phase BLDC motors: sensor and sensorless. The sensorless BLDC motor control approach is based on the Back Electromotive Force (BEMF) produced in the stator windings. The suggested CPLD- and BEMF-based Hybrid Commutation Model significantly outperforms traditional microcontroller-based, sensor-dependent BLDC motor control systems. The approach achieves the following goals by using BEMF for sensorless operation and a CPLD for high-speed logic processing: faster commutation transitions, higher efficiency, greater fault tolerance, and reduced torque ripple. Our realization is divided into three main sections. These sections are discussed in the methodology. This method uses hybrid commutation and sensorless feedback via the back electromagnetic field method. Plots of speed and motor current, the microcontroller's triggering pulses, and the MOSFET-manipulated BLDC motor input voltage have been shown. CPLD + BEMF-based Hybrid offers the best efficiency, seamless switching, and the highest torque ripple reduction (~45%), making it ideal for high-performance applications.

*Corresponding author.
E-mail address: singh.juli@gmail.com (S.J. Singh).
Peer Review under the responsibility of Universidad Nacional Autónoma de México.

Keywords: **BLDC-brushless DC motor, ECC-electronic controller circuit, PCB-printed circuit board, ZCD-zero cross detector, LCD-liquid crystal display, CPLD-complex programmable logic device, PWM- pulse width modulation.**

1. Introduction

A DC machine's main components are the commutator and brushes. A BLDC motor was developed to address the drawback of DC motors: brushes wear out under high-speed, high-current conditions. Due to their small size, high efficiency, and ability to operate at high speeds, BLDC motors are in high demand today. Therefore, a BLDC motor's performance is significantly superior to that of a DC motor (Ramachandra et al., 2019; Li et al., 2021). Brushless DC motors are rapidly replacing brushed DC motors in a wide range of applications, including electric fans, electric vehicles, drones, and medical equipment (Sadhique et al., 2019; Kumar & Singh, 2019). The architecture of the BLDC motor drive is continually improved by control and design engineers for a range of applications. The commutation mechanism explains a BLDC motor's primary function(Pindoriya et al., 2016). When the BLDC motor stator coils receive power from an external source and become electromagnets, they create a constant field in the air gap. The DC input power source for BLDC motors is switched to produce a trapezoidal AC voltage waveform. The rotor continues to rotate due to the forceful interaction between the permanent magnet rotor and the electromagnet stator(Pindoriya et al., 2016). A MOSFET is a type of electrical device in the field-effect transistor (FET) family. To switch MOSFETs, a driver circuit is used, and the microcontroller controls it. A MOSFET controls the switching signals, and a pulsating DC signal energizes the matching winding to create the North and South stator poles (*Pico-series Microcontrollers*, 2024). While using a microcontroller to adjust the speed of a brushless DC motor is a regular practice, VLSI (Very large scale integration) is used to fine-tune modern technology. The process of integrating thousands or millions of transistors or MOSFETs into a single chip is known as vector logic semiconductor integration, or VLSI. To address the aforementioned problems, a novel hybrid control strategy has been devised that blends the traditional Back EMF approach with an alternative approach using a microcontroller, a PID controller, and a CPLD. The Altera technique, which uses the MAX II Integrated Circuit, is used to fabricate CPLDs. With this IC, the electronic control circuit will function smoothly and reliably.To perform hybrid commutation, a positive voltage is applied to the motor input, and the motor starts running. At that time, the motor draws high current. If the motor starts normally or appears to rotate, it requires a lower duty cycle. If the duty cycle is not reduced or a constant PWM is used, the brushless DC motor will become very hot, and the MOSFET will also generate excessive heat. The motor's winding can also be damaged. Therefore, variable PWM pulses are given to the motor, which is controlled through the CPLD.

Many BLDC motor drive controls are Microcontroller-based, which suffer from drawbacks such as sequential program execution and high power consumption in battery-operated systems. This drawback can be mitigated by using a CPLD controller that supports parallel programming (i.e., multiple tasks run simultaneously), reducing execution time and power consumption, making it suitable for battery-operated systems. Therefore, a CPLD-based controller is used in this research.

2. Review of BLDC motor control schemes

There are two main control schemes for BLDC motor drives: sensor-based and sensorless. There are various sensor-based and sensorless methods for BLDC motor control. A Hall sensor and encoder are used in sensor-based BLDC motor control to locate the rotor magnet and provide a signal that suitably excites the stator winding. The Hall Effect, which states that a current-carrying conductor experiences a transverse force in a magnetic field, is the basis for how Hall sensors work. Large-power BLDC motors are typically built with integrated hall sensors (Pindoriya et al., 2016; Zhou et al., 2018).One drawback of a sensored BLDC motor is that installing the sensors requires additional space, and temperature variations can lead to inaccuracies in rotor position sensing (Ramachandra et al., 2019; Pindoriya et al., 2016).Sensorless operation of BLDC motors is usually achieved using back-EMF integration, artificial neural networks, third-harmonic methods, freewheeling-diode conduction, and trapezoidal back-EMF zero-crossing

approaches. Even at low speeds, the flux estimation approach is the most accurate method for determining rotor position because it is not speed-dependent, unlike the other three methods (Ramachandra et al., 2019; Li et al., 2021; Pindoriya et al., 2016). In unidirectional applications, like fans and pump loads, the Align & Go method is used to start a BLDC motor without first activating the rotor detection sensor. To maximize motor performance, every motor parameter needs to be adjusted during the align state, which depends on the motor phase resistance and the drain-source resistance of the FETs during the motor's on state (Pindoriya et al., 2016; Meghana & Singh, 2020).Additionally, a method for determining the zero crossing point of the Back EMF was described in order to improve stability and enable position-sensorless control of BLDC motors running at low speeds(Pindoriya et al., 2016; Damodharan & Vasudevan, 2010;Ju et al., 2014; Philip & Meenakshy, 2012; Rao & Taib, 2008; Li & Zhou, 2018; Damodharan & Vasudevan, 2010). The independent speed amount G function is used by the three proposed algorithms to effectively locate the zero-crossings of line-to-line back EMF. The speed calculation method represented the second technological achievement, while the commutation error correction algorithm represented the third(Li & Zhou, 2018). Without sensors, one of the many uses for DC motors is in solar photovoltaic (PV) irrigation systems with water pumps(Kumar & Singh, 2019).A low-cost three-phase trapezoidal back-emf permanent magnet BLDC motor drive for variable-torque, constant-speed applications, using a microcontroller-based 120-degree six-step control algorithm (Mukherjee et al., 2013). This has been achieved by using a straightforward buck converter topology to regulate the voltage. The PIC16F877A microcontroller's built-in Pulse Width Modulation (PWM) capability has been used in buck converters (Mukherjee et al., 2013). The electronics speed controller in this system receives pulse-width modulation (PWM) signals from the ATMEGA controller and then switches its solid-state components in accordance with the BLDC motor switching logic (Rao & Taib, 2008). The use of the PWM control technique for speed control of BLDC motors. The paper highlights the importance of proper heat management in BLDC motor control systems(Anshory et al., 2024). The whole power and control circuit is powered by solar energy. Using a boost converter, the solar panel provides the system with a controlled and necessary power supply (Kumar & Singh, 2019; Gupta & Pandey, 2012). The BLDC motor's speed is controlled by a PIC microcontroller, which adds bulk and weight to the system because it requires additional hardware. Instead, FPGA offers an efficient speed control solution that requires less hardware. VHDL is the programming language used to design the Spartan-3 FPGA kit (Giridharan & Gautham, 2013; Zoheb et al., 2013). Using the program's pluses and gate pulses, the MOSFETs of a three-phase fully regulated bridge circuit operate a BLDC motor drive (Zoheb et al., 2013; Suneeta et al., 2016; Tashakori et al., 2015). The Xilinx FPGA SPARTAN-3A training kit and the digital PWM Generator topology are used to simulate the integrated BLDC motor(Zoheb et al., 2013; Tashakori et al., 2015; Sathyan et al., 2009). Likewise, FPGA boards using a PWM speed controller, the Spartan 3E control drive for BLDC motors, have been demonstrated (Tashakori et al., 2015). This method of controlling BLDC motors uses three built-in Hall-effect sensors to detect rotor position and then applies a PWM signal to the upper-side switches of the inverter, or the user can do it manually (Tashakori et al., 2015). To regulate the speed of BLDC motors, a CPLD is also used alongside an FPGA. Using Max II EPM240T100C5 devices, the control technique presented in this study was applied to a 350W, 36 V-rated BLDC motor to generate the PWM signal. In the commutation process, the rotor position is ascertained using the inbuilt Hall sensor. The proposed method designs the BLDC motor using CPLD. Since the CPLD is a non-volatile device, it does not require programming or configuration when the system restarts(Sachruddin et al., 2021). Theoretical Gaps: current research lacks a comprehensive hybrid commutation technique that effectively combines BEMF-based sensorless operation at low speeds with CPLD for real-time adaptive control. (Pindoriya et al., 2016; Damodharan & Vasudevan, 2010)

Practical Gaps: An improved CPLD-based hybrid commutation system with adaptive switching and SVPWM integration is needed because current-sensorless BLDC systems exhibit poor low-speed performance, long response times, and significant torque ripple (Alshehabi et al., 2012).

It was clear from the study papers how the speed regulation and commutation of the BLDC motor were achieved. More progress has been made in this field; in this work, a new design technique using CPLD Max II is employed to achieve commutation and speed control of BLDC motors. The experimental configuration is shown in Figure 3 of the suggested procedure. The six IRF540 MOSFETs in the BLDC motor are rated for 48V, 500 rpm, and 500W. An ESC controller circuit and a limiting resistance link the BLDC motor to the CPLD.

3. Methodology

The BLDC motor suggested in this work is used in electric cars; in these cars, the gearbox has been discarded because our hardware does not require it. There are three primary parts to our hardware realization. The first component is utilizing an RP2040 Raspberry Pi Pico W microcontroller. The pulse width modulation (PWM) frequency, duty cycle, voltage, current, and other system characteristics can be measured, and the rotation speed and direction can be adjusted. The second component is a complex programmable logic device (CPLD) that uses PWM input to generate a three-phase sequence. Hardware is designed and realized using a CPLD. A BLDC motor driver is the third component. The driver circuit uses an IRF540 MOSFET and an IR2104S half-bridge driver. This BLDC motor can run at 48 volts, 13.4 amps, and 500 watts. Our project's hardware now uses a 24-volt, 10-amp supply because a 48-volt source was unavailable.

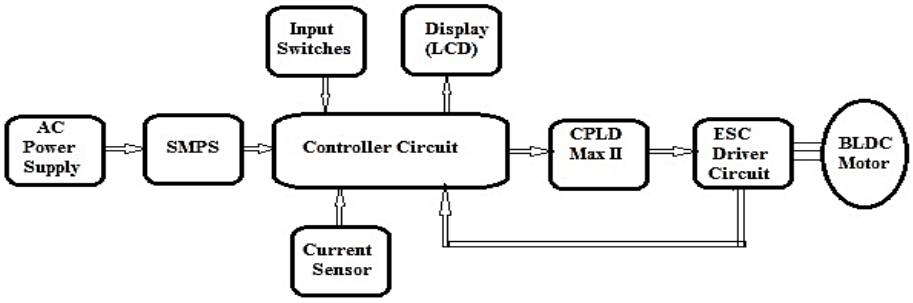

Figure 1. Block diagram of ECC-based three-phase sensorless BLDC motor drive.

In the block diagram depicted in Figure 1, the fundamental connections between these ESC sections and a sensor-less BLDC motor that uses electronic hybrid commutation are indicated.

An Electronic speed Controller (ESC) is used in a standard printed-circuit-board-based brushless motor control system. An SMPS + battery power supply, a RIP 2040 PIC microcontroller, a CPLD (Max-II), a Hall sensor for the current sensor, a three-phase ESC driver circuit, and line sensors are all included in this ESC.

The block diagram of a three-phase sensorless BLDC motor drive is shown in Figures 2 (a), (b), (c), and (d). It is clear from these that each section of the block diagram of a brushless DC motor includes a detailed explanation of the circuit and highlights the key components of the power supply, controller circuit, current sensor, LCD display, and CPLD MAX-II Block, as well as the ESC Drive circuit.

Table 1 Components used in hardware.

SN	Components	Data Set	QTY
1	Power Supply	SMPS 24 V, 10AMP	1
2	Microcontroller	RPI2040 PICO	1
3	Current Sensor	ACS712	2
4	CPLD	Altera MAX II	1
5	LCD	16X2 WITH 16 PIN	1
6	MOSFET	IRF540	3
7	Half Bridge Driver	IR2104S	3
8	Amplifier	LM358	2
9.	Battery	24 V, 1.35 A	3
10	Buck Boost Converter	5V	1
11	Buck Boost Converter	12 V	1

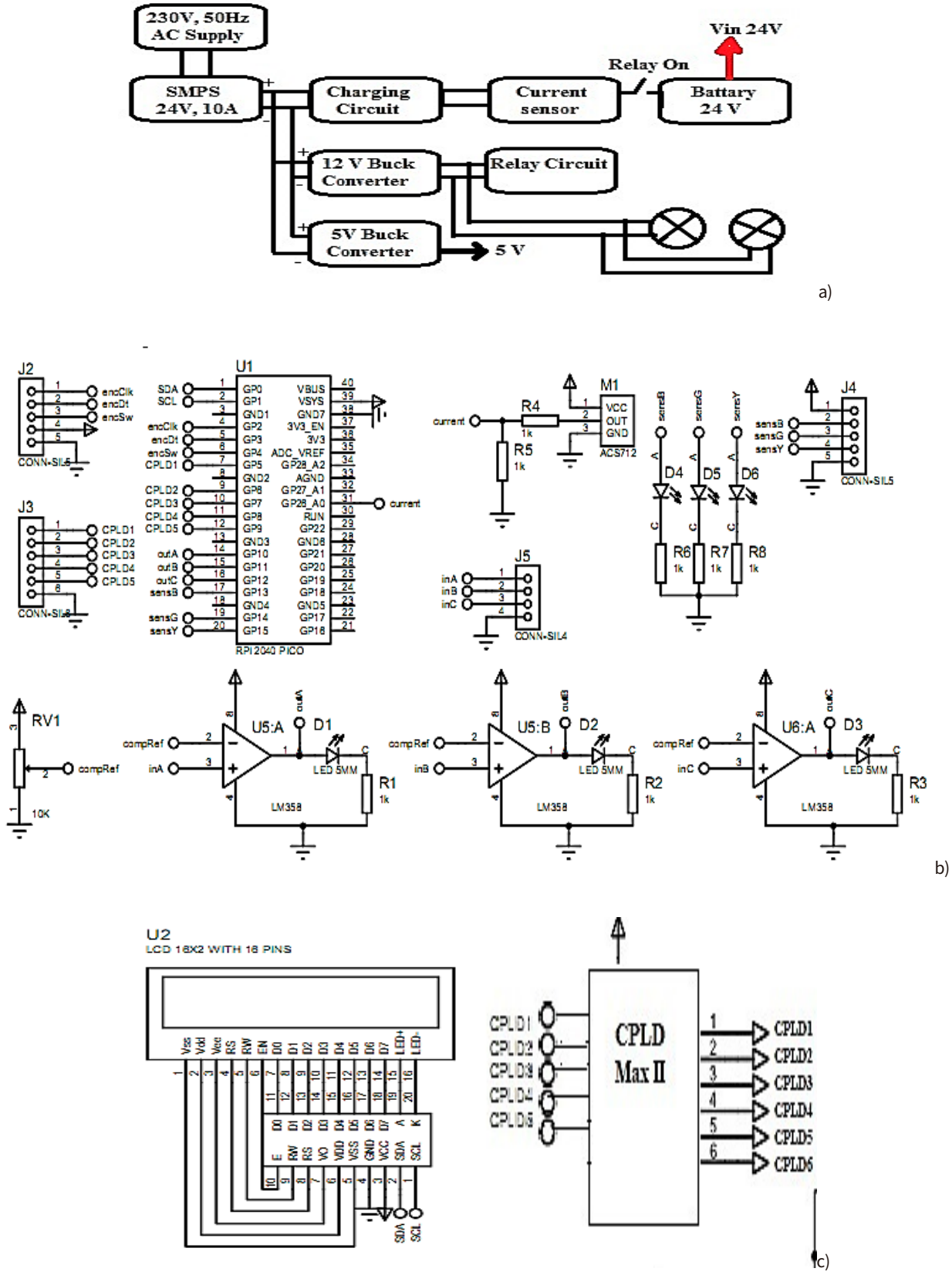

Figure 2: (a) Power supply; (b) Controller circuit and current sensor; (c) LCD Display and CPLD MAX –II block.

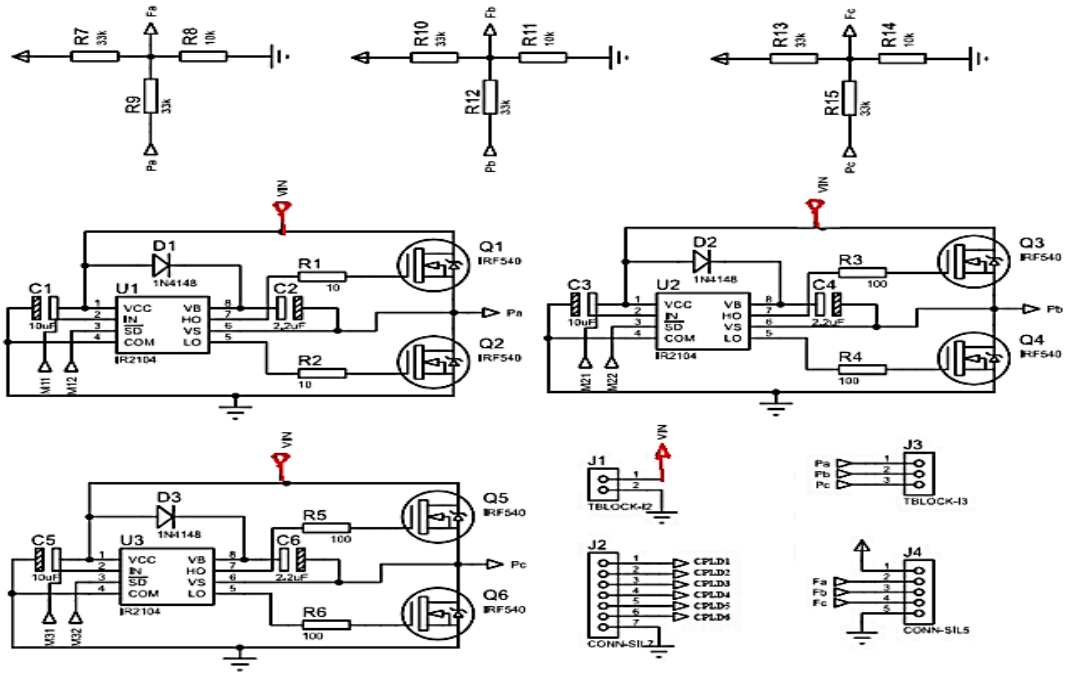

d)

Figure 2: d) ESC Drive circuit.

4. An overview of each block in a block diagram

As shown in Figures 1 and 2(a), the SMPS requires a 230 V, 50Hz input. 230 VAC is converted into 24 VDC at 10 A using an SMPS. A 5-volt buck converter converts 24-volt DC to 5-volt DC. The CPLD Max II board (Figure 2(c)), the ESC driver (Figure 2(d)), the controller circuit (Figure 2(b), and other electronic devices are powered by 5-volt DC. The controller circuit uses a microcontroller (Figure 2(b), an LCD (Figure 2(c)), a hall current sensor (Figure 2(b)), and five push buttons (Figure 2(d)). The current sensor detects whether current is flowing through the circuit and notifies the microcontroller if the motor draws excessive current. The CPLD Max II board receives PWM pulses generated in accordance with motor current via the microcontroller's code. The CPLD Max II generates a PWM signal that the ESC driver circuit uses to switch the MOSFET. A balanced three-phase input is supplied to the BLDC motor via a switching pattern that produces a 120° phase shift between the input voltage phases. As a result, the motor operates smoothly and efficiently.

4.1 Electronic speed controller

A sensorless BLDC motors rely on the BEMF (Back Electromotive Force) generated in the stator windings for commutation, eliminating the need for rotor position sensors. Actually, large-power-rating BLDC motors come with built-in Hall sensor connectors. Whether to use the BLDC motor's Hall sensor terminal is up to the client (How Brushless DC Motor Works?). *(BLDC and ESC Explained*, 2024; Tang & Cui, 2013). Each of the BLDC motor's three windings produces BEMF when it turns, which opposes the main voltage. Similar to the signals produced by the CPLD Max II, the three BEMF signals that are generated are 120° out of phase. The link between the CPLD output signals and the BEMF signals is depicted in Figure 3:

Totally, there are 6 events:

- Phase R zero crossing:
  - –from high to low and
  - –from low to high
- Phase Y zero crossing:
  - –from high to low and
  - –from low to high
- Phase B zero crossing:
  - –from high to low and
  - –from low to high

The BLDC motor's BEMF zero-crossing points can be found most easily using LM358 (ZCD) comparators. A positive terminal, a negative terminal, and an output are the comparator's three main terminals. The comparator output indicates which is higher: the negative voltage or

the positive voltage. It is logic high for a higher positive voltage and logic low for a lower positive voltage. ZCD circuits, commonly called comparators, are required for this project.

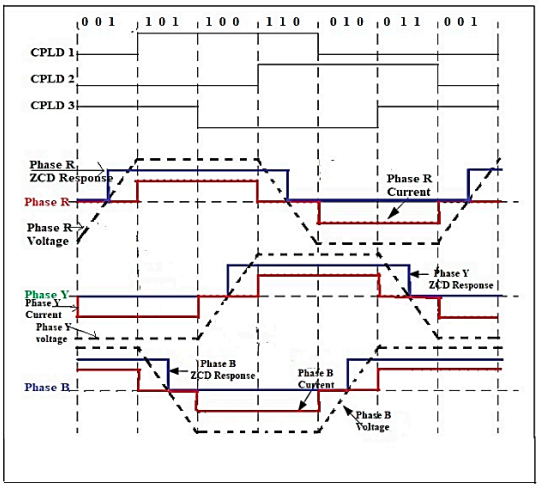

Figure 3. Relationship between CPLD Max – II out signals and the BEMF signals.

As shown in Figure 4, three resistors form the virtual natural point N'(Yu, 2017; *MOSFET*). This procedure is repeated for three comparators. The comparator output changes from low to high due to the BEMF produced in the floating (open) winding, shifting from the negative to the positive side. The comparator output changes from high to low when the BEMF produced in the floating winding passes the zero line and moves towards the negative side. Three of these comparator circuits—one on each phase—produce three digital signals that represent the BEMF in the windings (Sachruddin et al., 2021). These three signals from the CPLD are combined to produce the commutation sequence.

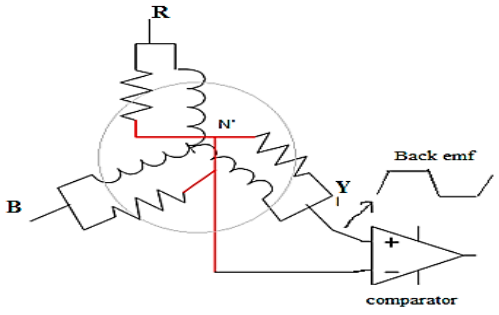

Figure 4. Comparators connection for the BLDC motor for each phase.

5. Hardware setup

The hardware implementation of the sensorless BLDC motor drive control using Hybrid Commutation (CPLD + BEMF) is divided into three main blocks, as illustrated in Figures represents 1(a) power supply, 1(b) controller circuit and current sensor, 1(c) LCD display and CPLD Max –II block, and 1(d) ESC Drive circuit.

5.1 BLDC Motor Control Circuit

This block is responsible for processing sensorless control algorithms, managing system feedback, and displaying real-time motor performance parameters. The key components include:

Table 2.Hardware components and their functions

Component	Function
5V Buck Converter	Provides a stable 5V DC power supply for control circuits.
Microcontroller (RIP2040 PIC)	Executes control logic, speed regulation, and real-time data processing.
LCD Display (20x4, 18 Pins)	Displays speed, current, and system status in real-time.
Dual Operational Amplifier (LM358)	Used as a comparator for zero-cross detection of BEMF signals.
Current Sensor (ACS712)	Measures motor phase current for protection and feedback control.
3-Color (5mm) LED Indicators	Provides visual feedback on system operation and fault detection.

5.2. Three-phase driver circuit

This block controls the power transistors that drive the BLDC motor. It includes:

Table 3. Three-phase drives circuits, components, and their function

Component	Function
Half-Wave Bridge Rectifier(IC IR2104)	Drives the MOSFETs in a three-phase bridge configuration.
MOSFET (IRF540)	Acts as the power switch to control motor phases.
Diode (1N4148)	Provides flyback protection to prevent voltage spikes.
Resistors (High & Low Power Values)	Used for gate drive control, voltage division, and current limiting.

5.3. CPLD MAX-II block -

The Complex Programmable Logic Device (CPLD) MAX-II serves as the core high-speed control unit, responsible for real-time generation of commutation signals and logic processing. Its functions include:

Table 4. CPLD MAX –II block components and their function.

Component	Function
CPLD MAX-II (Altera)	Generates precise switching signals for the electronic control circuit.
Signal Conditioning Circuit	Filters and conditions BEMF signals for accurate zero-cross detection.
Fault Handling Mechanism	Monitors system parameters and initiates protective actions during faults.

Figure 5 represents the hardware setup, and 1 to 8 represent hardware components, respectively, which are as follows:

(1) 24V, 10A SMPS (Power supply) (2) 6V battery (3) Battery charging circuit (4) Micro Controller Circuit and LCD (5) Push buttons (6) Fans for cooling MOSFETS (7) Electronics Speed control circuit (8) CPLD Max-II IC (9) Brushless DC motor.

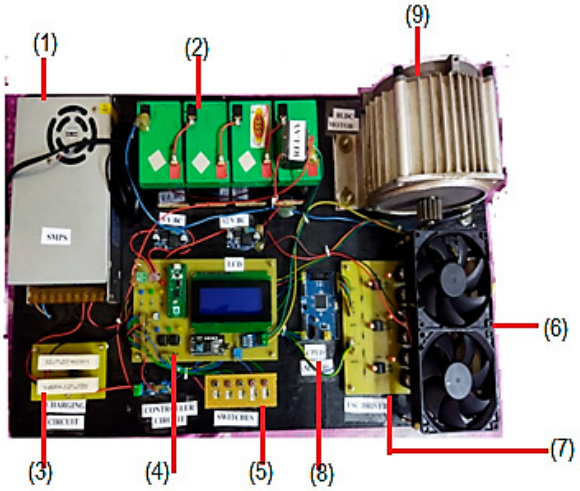

Figure 5. Hardware setup.

5.4 Hardware system overview

The BLDC motor control system integrates these three main blocks to provide hybrid commutation using CPLD and BEMF, as shown in Figure 5, ensuring:

- Fast commutation response (<6 µs) via CPLD logic processing.
- Seamless low-to-high speed transition
- Efficient power switching with IRF540 MOSFETs.
- Real-time performance monitoring via LCD and LED indicators.

6. Results and Discussion

Figure 6 shows the voltage-time waveform of the BLDC motor at different speeds. It is also similar, with minimum and maximum speed conditions such as 50, 100, 200, 300, and 400 rpm.

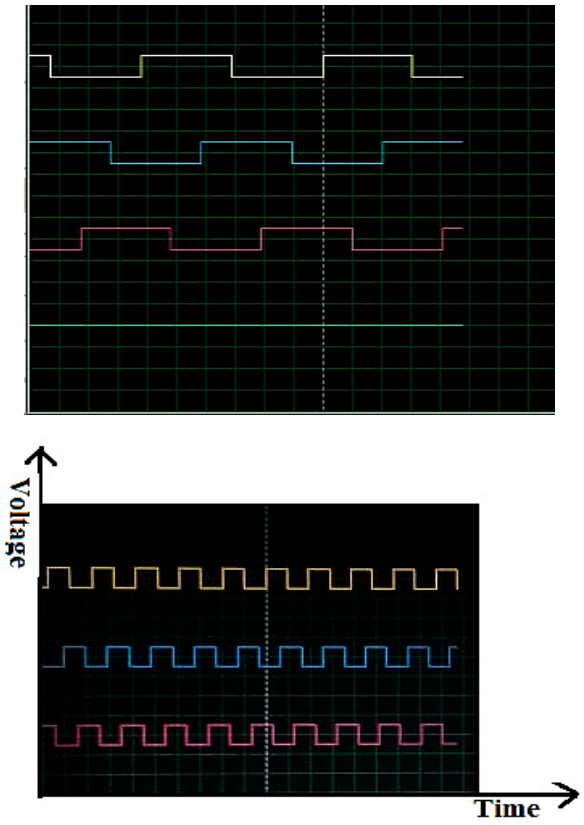

Figure 6. Microcontroller output in pulse form, with a minimum of 50 rpm and a maximum of 400 rpm.

The waveform above shows the Digital storage oscilloscope output of the Rip2040 microcontroller fed into the ESC drive circuit of the sensorless BLDC motor drive. To generate a pulse output from a microcontroller to control a BLDC motor, this technique is called Pulse Width Modulation (PWM).

In general, at low speeds, the voltage waveform applied to a BLDC motor would be more trapezoidal in nature (Figure 7). This means the motor windings are energized to produce a trapezoidal back-emf waveform, characteristic of BLDC motors operating in a trapezoidal commutation mode.

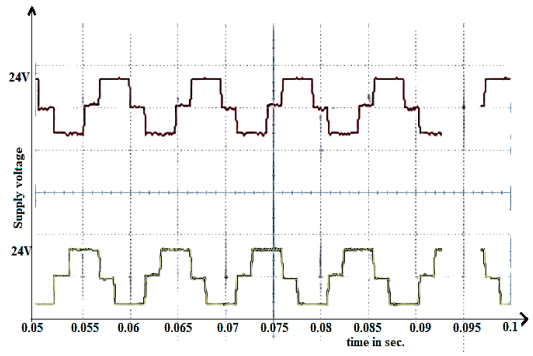

Figure 7. Voltage and time waveform of the BLDC motor at 50 rpm.

The voltage waveform of a Brushless DC (BLDC) motor at 50 rpm depends on factors such as the motor design, the number of poles, the winding configuration, and the control strategy used (e.g., trapezoidal commutation).

Figure 8 shows a voltage and time waveform for a BLDC motor at 100 RPM. A simplified scenario in which the motor is driven by a trapezoidal commutation strategy is assumed. In this strategy, the voltage applied to each motor phase varies trapezoidally over time.

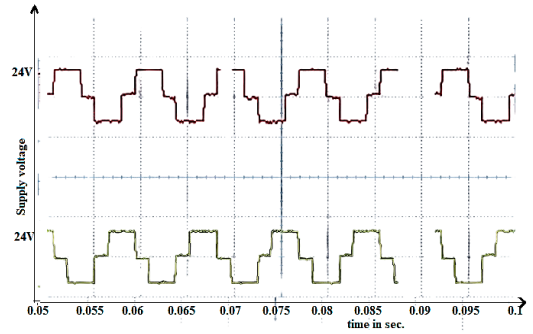

Figure 8. Voltage and time waveform of the BLDC motor at 100 rpm.

At 100 rpm, the motor rotates at a relatively low speed, so the voltage waveform applied to the motor will resemble a trapezoid. Here's a simplified explanation of what the voltage waveform might look like:

1. **Phase Energization:** In a typical trapezoidal commutation scheme, the motor phases are energized sequentially in a specific order as the rotor rotates. Let's say we have three motor phases labeled A, B, and C.
2. **Voltage Application:** At any given time, one phase is energized with a positive voltage, another phase with a negative voltage, and the third phase is either floating or connected to the neutral point. The exact timing and duration of each voltage phase depend on the motor design and the desired speed.
3. **Waveform Shape:** The voltage waveform applied to each phase will have a rising edge, a plateau (where the voltage remains constant), and a falling edge as the commutation occurs.

Without specific motor parameters and controller settings, it's challenging to provide an exact waveform. This representation shows a simplified trapezoidal waveform where the voltage rises, remains constant for a period (while the motor phase is energized), and then falls. The pattern repeats as the motor rotates.

Figure 9 shows that at 200 RPM, the voltage waveform applied to a BLDC motor would still be trapezoidal in nature, but the frequency of commutation would increase compared to lower speeds. This means that the duration of each phase's energization and the intervals between commutation events would be shorter.

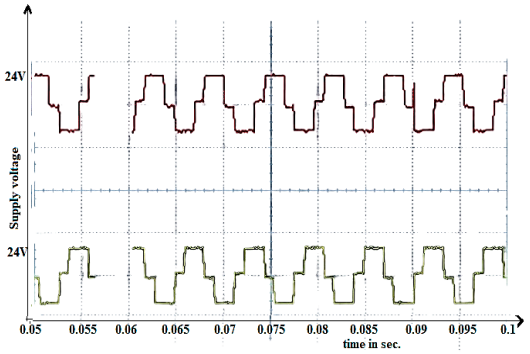

Figure 9. Voltage and time waveform of the BLDC motor at 200 RPM.

In this waveform:

- Each phase is energized with a positive voltage for a certain duration.
- The voltage remains relatively constant during the energization period.
- After the energization period, there's a short interval (commutation time) before the next phase is energized.
- The waveform repeats as the motor rotates.

The actual implementation details depend on the Rip2040 microcontroller and the programming languages used.

Figure 10 shows that as the BLDC motor speed increases to 300 rpm, the commutation frequency further increases, resulting in shorter phase-energization durations and shorter intervals between commutation events. Here's a general representation of the voltage and time waveform for a BLDC motor operating at 300 rpm.

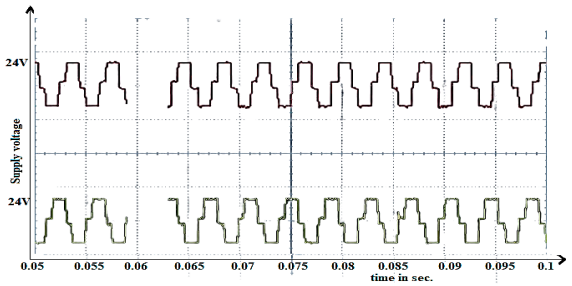

Figure 10. Voltage and time waveform of the BLDC motor at 300 rpm.

Figure 11 shows that as the BLDC motor speed increases to 400 rpm, the commutation frequency continues to rise, resulting in even shorter phase-energization durations and shorter intervals between commutation events. Here is a general representation of the voltage and time waveform for a BLDC motor operating at 400 rpm.

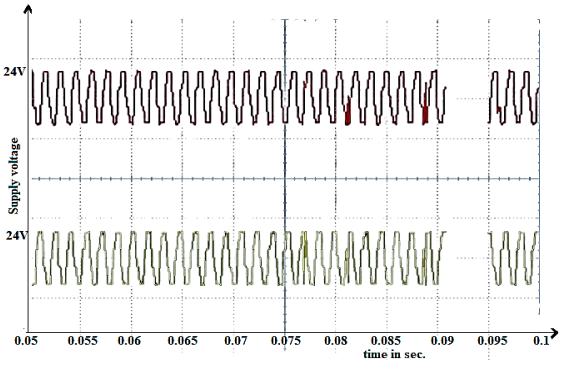

Figure 11. Voltage and time waveform of the BLDC motor at 400 rpm.

Figure 12 shows the voltage and time waveform of a three-phase BLDC (Brushless DC) motor, which typically involves sequentially energizing the motor phases to create a rotating magnetic field that drives the motor's rotation. Let's consider a simplified trapezoidal commutation scheme for a three-phase BLDC motor.

In a simplified representation, during each electrical cycle (360 electrical degrees), two phases are energized while the third phase remains floating.

In this waveform:

- Each section represents one electrical cycle.
- Phases A, B, and C are represented by their respective waveforms.
- During each electrical cycle, two phases are energized with positive and negative voltages, while the third phase remains floating.
- The voltage waveforms are typically trapezoidal in shape, with each phase having a rising edge, a plateau where the voltage remains constant, and a falling edge.

The exact timing and duration of each phase's energization depend on the motor's rotor position, speed, and the commutation strategy being employed. This simplified representation illustrates the basic concept of trapezoidal commutation in a three-phase BLDC motor.

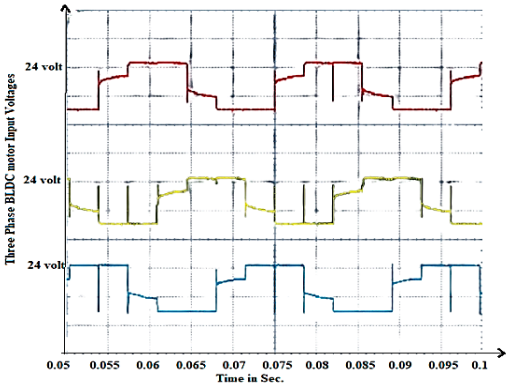

Figure 12. Three-phase voltage and time waveform of BLDC motor.

6.1 Experimental result analysis in tabular form

Supply voltage =24 volt
Dir (Direction of motor rotation) -
CW (clockwise)/ACW (counterclockwise)
USP(Motor set speed) in rpm
I_m (motor current) in Amp
I_c (Charging current) in Amp
MSP (Motor actual speed) in rpm

Table 4 shows that the BLDC motor exhibits the least variation in current across speed settings when supplied with a constant 24 volts. By examining the table,

one may understand that the motor current decreases as one stares. The motor's current grows in tandem with its speed, so the current value varies relatively little. Table 5 shows less variation in motor current than in speed, indicating that even under varying load conditions, BLDC motor efficiency increases. The BLDC motor draws a high current through the current sensor under load, providing feedback to the microcontroller that can be controlled via the PRM signal. These sensors detect smaller current variations because the motor's commutation is managed by a hybrid commutation method.

Table 5. Speed analysis in tabular form.

S.N.	USP	I_m	I_c	Dir	MSP
1	at start	2.8	1.3	CW/ACW	0
2	50	4.2	3.1	CW/ACW	50
3	100	4.0	3.1	CW/ACW	88
4	200	3.8	3.1	CW/ACW	188
5	300	3.8	3.1	CW/ACW	288
6	400	3.2	3.1	CW/ACW	388

Table 6 presents a comparative analysis of our proposed work with traditional methods mentioned in the referenced papers. We can clearly see a significant improvement in the Brushless DC motor's performance by using a CPLD + BEMF hybrid commutation.

Table 6.Comparative study of hybrid commutation techniques.

Technique	Hall Sensor + BEMF	Forced Commutation + BEMF	CPLD + BEMF based Hybrid
Low-Speed Operation	Stable	Moderate Stability	Fast Response
High-Speed Performance	High Efficiency	Effective	Seamless Switching
Efficiency	Medium	Medium	High
Complexity	Low	Low	Medium
Torque Ripple Reduction	Moderate	Moderate	High (~45%)

7. Conclusions

Implications of the Research is the CPLD processes BEMF signals with minimal latency, optimizing phase commutation, Hybrid commutation minimizes torque ripples, reducing mechanical stress and power losses, ensures smooth transitions between the two modes low and high speed performance, parallel processing capabilities, enabling real-time motor control without significant delays and CPLD-based controllers are compact and field-reprogrammable, allowing for real-time updates and custom optimizations. The integration of CPLD-based control and BEMF hybrid commutation considerably boosts BLDC motor performance. This research illustrates how CPLDs provide real-time, high-speed processing for efficient commutation, while BEMF detection enables sensorless operation at greater speeds. The combined technique enhances motor efficiency, lowers torque ripple, and ensures robust fault tolerance. Electric vehicles (EVs) and hybrid electric vehicles (HEVs), drones and aircraft, industrial automation and robotics, clean energy systems, and healthcare technology are among the possible uses of hybrid commuting.

Finally, this paper describes the components used for hardware implementation and how they were assembled in detail.

For future scope, systems such as fuzzy logic or AI can be combined with a CPLD to enable hybrid technology in a brushless DC motor. This can further improve the performance or efficiency of a brushless DC motor.

Conflict of interest

The authors have no conflict of interest to declare.

Funding

The authors received no specific funding for this work.

References

Alshehabi, A., Ferdowsi, M. H., & Pahlavani, M. A. (2012). Improving the Performance of Brushless DC Motor Using the Six Digits form of SVPWM Switching Mode.

Anshory, I., Wisaksono, A., Jamaaluddin, J., & Fudholi, A. (2024). Implementation of ARM STM32F4 microcontroller for speed control of BLDC motor based on bat algorithm. *International Journal Of Power Electronics And Drive Systems*, *15*(1), 127-135.

Damodharan, P., & Vasudevan, K. (2010). Sensorless brushless DC motor drive based on the zero-crossing detection of back electromotive force (EMF) from the line voltage difference. *IEEE Transactions on Energy Conversion*, *25*(3), 661-668. https://doi.org/10.1109/TEC.2010.2041781

Damodharan, P., & Vasudevan, K. (2010). Sensorless brushless DC motor drive based on the zero-crossing detection of back electromotive force (EMF) from the line voltage difference. *IEEE Transactions on Energy Conversion*, *25*(3), 661-668. https://doi.org/10.1109/tec.2010.2041781

Giridharan, K., & Gautham, R. (2013). FPGA Based Digital Controllers for BLDC Motors. *International Journal of Engineering research and applications*, 1615-1619.

Gupta, N and Pandey, D." A Review: Sensorless Control of Brushless DC Motor;,," in Esrsa Publications: Auckland,, New Zealand, 2012.

How Brushless DC Motor Works? BLDC and ESC Explained. (2024). https://howtomechatronics.com/how-it-works/how-brushless-motor-and-esc-work/

Ju, L. C., Wang, Z. Q., & He, M. Y. (2014). Design and Research of a Sliding Mode Observer Based on Line Back-EMF for Brushless DC Motors. *Applied Mechanics and Materials*, *615*, 11-17. https://doi.org/10.4028/www.scientific.net/AMM.615.11

Kumar, R., & Singh, B. (2019). Solar PV powered-sensorless BLDC motor driven water pump. *IET Renewable Power Generation*, *13*(3), 389-398. https://doi.org/10.1049/iet-rpg.2018.5717

Li, T., & Zhou, J. (2018). High-stability position-sensorless control method for brushless DC motors at low speed. *IEEE transactions on power electronics*, *34*(5), 4895-4903. https://doi.org/10.1109/TPEL.2018.2863735

Li, Y., Wu, H., Xu, X., Sun, X., & Zhao, J. (2021). Rotor position estimation approaches for sensorless control of permanent magnet traction motor in electric vehicles: A review. *World Electric Vehicle Journal*, *12*(1), 9. https://doi.org/10.3390/wevj12010009

Meghana, R. R. S. R., & Singh, R. R. (2020). Sensorless start-up control for BLDC motor using initial position detection technique. In *2020 IEEE International Conference on Power Electronics, Smart Grid and Renewable Energy (PESGRE2020)* (pp. 1-6). IEEE.

MOSFET Amplifier. (s. f.). https://www.electronics-tutorials.ws/amplifier/mosfet-amplifier.html,»

Mukherjee, A., Ray, S., & Das, A. (2013). Microcontroller Based Constant Speed Low Cost Energy Efficient BLDC Motor Drive Using Proteus VSM Software.

Philip, P., & Meenakshy, K. (2012). Modelling of brushless dc motor drive using sensored and sensorless control (back emf zero crossing detection). *International Journal of Emerging Technology and Advanced Engineering, ISSN 2250-2459*, *2*(8).

Pico-series Microcontrollers. (2024). https://www.raspberrypi.com/documentation/microcontrollers/pico-series.html

Pindoriya, R. M., Mishra, A. K., Rajpurohit, B. S., & Kumar, R. (2016). Analysis of position and speed control of sensorless BLDC motor using zero crossing back-EMF technique. In *2016 IEEE 1st International Conference on Power Electronics, Intelligent Control and Energy Systems (ICPEICES)* (pp. 1-6). IEEE. https://doi.org/10.1109/ICPEICES.2016.7853072

Ramachandra, Y., Akhileshwar, M., Pandian, A., Nalli, R., & Subbarao, K. (2019). Analysis of recent developments in brushless DC motors controlling techniques. *Int J Innov Technol Explor Eng*, *8*(5), 522-526.

Rao, K. R., & Taib, S. (2008). Sensorless control of a BLDC motor with back EMF detection method using DSPIC. In *2008 IEEE 2nd International Power and Energy Conference* (pp. 243-248). IEEE.

Sachruddin, M. F., Samman, F. A., & Sadjad, R. S. (2021). BLDC motor control using a complex programmable logic device with hall-sensors. In *2021 International Conference on Smart-Green Technology in Electrical and Information Systems (ICSGTEIS)* (pp. 7-11). IEEE. https://doi.org/10.1109/ICSGTEIS53426.2021.9650433

Sachruddin, M. F., Samman, F. A., & Sadjad, R. S. (2021). BLDC motor control using a complex programmable logic device with hall-sensors. In *2021 International Conference on Smart-Green Technology in Electrical and Information Systems (ICSGTEIS)* (pp. 7-11). IEEE. https://doi.org/10.1109/ICSGTEIS53426.2021.9650433

Sadhique, M. J., Ashok, S., Sandeen, J., & Deepthi, S. (2019). Position sensorless control for BLDC motor for powertrain applications. In *2019 2nd International Conference on Intelligent Computing, Instrumentation and Control Technologies (ICICICT)* (Vol. 1, pp. 322-327). IEEE. https://doi.org/10.1109/ICICICT46008.2019.8993184

Sathyan, A., Milivojevic, N., Lee, Y. J., Krishnamurthy, M., & Emadi, A. (2009). An FPGA-based novel digital PWM control scheme for BLDC motor drives. *IEEE transactions on Industrial Electronics*, *56*(8), 3040-3049. https://doi.org/10.1109/TIE.2009.2022067

Suneeta, S., Srinivasan, R., & Sagar, R. (2016). FPGA based control method for three phase BLDC motor. *International Journal of Electrical and Computer Engineering*, *6*(4), 1434.

Tang, N and Cui, B. (2013) " A high resolution detecting method for rotor zero initial position of sensorless brushless DC motor," Trans. *China Electrotech, p. 90–96., Soc.*

Tashakori, A., Hassanudeen, M., & Ektesabi, M. (2015). FPGA based controller drive of BLDC motor using digital PWM technique. In *2015 ieee 11th international conference on power electronics and drive systems* (pp. 658-662). IEEE.

Yu, C. H. (2017). A practical sensorless commutation method based on virtual neutral voltage for brushless DC motor. *IEEJ Transactions on Electrical and Electronic Engineering*, *12*(5), 770-777.
https://doi.org/10.1002/tee.22464

Zhou, X., Zhou, Y., Peng, C., Zeng, F., & Song, X. (2018). Sensorless BLDC motor commutation point detection and phase deviation correction method. *IEEE Transactions on Power Electronics*, *34*(6), 5880-5892.
https://doi.org/10.1109/TPEL.2018.2867615

Zoheb, M., Sharma, M. V., Vashishtha, S., & Shahid, M. (2013). Implementation of brushless DC motor using FPGA interface. *International Journal of Engineering Research & Technology*, *2*(5), 12.